



OPEN ACCESS

EDITED BY Chiranjib Pal, West Bengal State University, India

REVIEWED BY
Maria Agallou,
Pasteur Hellenic Institute, Greece
Ruchishree Konhar,
Council of Scientific and Industrial Research
(CSIR), India

*CORRESPONDENCE Belén Vicente ☑ belvi25@usal.es Antonio Muro ☑ ama@usal.es

RECEIVED 27 August 2025
ACCEPTED 31 October 2025
PUBLISHED 25 November 2025

CITATION

Sánchez-Montejo J, Teodosio C, Strilets T, López-Abán J, Manzano-Román R, Pozo J, Martin S, Silos L, Trujillo I, García-Blanco MA, Vicente B and Muro A (2025) Harnessing mRNA technology against *Fasciola* hepatica: Immunological insights from a fatty acid binding protein vaccine. Front. Immunol. 16:1693674. doi: 10.3389/fimmu.2025.1693674

COPYRIGHT

© 2025 Sánchez-Montejo, Teodosio, Strilets, López-Abán, Manzano-Román, Pozo, Martin, Silos, Trujillo, García-Blanco, Vicente and Muro. This is an open-access article distributed under the terms of the Creative Commons Attribution License (CC BY). The use, distribution or reproduction in other forums is permitted, provided the original author(s) and the copyright owner(s) are credited and that the original publication in this journal is cited, in accordance with accepted academic practice. No use, distribution or reproduction is permitted which does not comply with these terms.

Harnessing mRNA technology against *Fasciola hepatica*: Immunological insights from a fatty acid binding protein vaccine

Javier Sánchez-Montejo¹, Cristina Teodosio^{2,3,4,5,6}, Tania Strilets⁷, Julio López-Abán¹, Raúl Manzano-Román¹, Julio Pozo^{4,8}, Silvia Martin^{4,6}, Lidia Silos⁶, Ignacio Trujillo¹, Mariano A. García-Blanco^{7,9}, Belén Vicente^{1*} and Antonio Muro^{1*}

¹Infectious and Tropical Diseases Research Group (e-INTRO), Biomedical Research Institute of Salamanca, Research Centre for Tropical Diseases at the University of Salamanca Instituto de Investigación Biomédica de Salamanca (IBSAL) - Centro de Investigación de Enfermedades Tropicales de la Universidad de Salamanca (CIETUS), Salamanca, Spain, ²Cancer Research Center Instituto Universitario de Biología Molecular y Celular del Cancer, Universidad de Salamanca - Consejo Superior de Investigaciones Científicas (IBMCC, USAL-CSIC), Salamanca, Spain, ³Department of Medicine, University of Salamanca (USAL), Salamanca, Spain, ⁴Cytometry Service (NUCLEUS), University of Salamanca (USAL), Salamanca, Spain, ⁵Centro de Investigación Biomédica en Red Cáncer (CIBERONC; CB16/12/00400), Madrid, Spain, °Biomedical Research Institute of Salamanca (IBSAL), Salamanca, Spain, ³Department of Microbiology, Immunology and Cancer Biology, University of Virginia, Charlottesville, VA, United States, °Cytognos SL, A BD Biosciences Company, Salamanca, Spain, °Center for RNA Science and Medicine, University of Virginia, Charlottesville, VA. United States

mRNA platforms offer a promising strategy to overcome limitations in helminth vaccinology. We used the helminth Fasciola hepatica, which is a major veterinary and zoonotic pathogen for which no licensed vaccine exists, as a test case. We engineered a codon-optimized mRNA encoding the F. hepatica fatty-acidbinding protein (FABP), verified its expression in HEK293T cells, and formulated it in SM-102 lipid nanoparticles (LNPs). BALB/c mice received a prime-boost immunization (3 weeks apart) followed by longitudinal blood and terminal spleen immune profiling by spectral flow cytometry. Immunization induced rapid innate immune activation with marked neutrophil expansion and monocyte maturation, while reducing circulating mature NK cells, consistent with recruitment to lymphoid tissues. Adaptive responses included increased circulating CD8⁺ T cells dominated by EMRA effectors, expansion of $TCR\alpha\beta+$ double-negative T cells with memory/effector phenotypes, and a reduction in peripherally induced CD25- regulatory T cells. CD4⁺ T-helper cells showed a shift toward memory/ effector subsets, and antigen-specific Th1 and Th2 responses in the spleen were detected only in vaccinated mice. B-cell analysis revealed accelerated maturation of B2 cells with expansion of marginal-zone, follicular, and germinal-center compartments, higher frequencies of class-switched (IgM-)

plasma cells, and exclusive detection of anti-FABP IgG in the mRNA-LNP group. These results demonstrate that an mRNA-LNP vaccine encoding *F. hepatica* FABPs elicits innate immune activation, cytotoxic and helper T-cell immunity, and class-switched humoral responses in mice, supporting its potential as a candidate for *F. hepatica* vaccination in a future challenge experiment against the infection.

KEYWORDS

Fasciola hepatica, parasite, trematode, mRNA vaccine, cytometry, FABP

1 Introduction

Fasciola hepatica, commonly known as the liver fluke, is a widespread endoparasite that infects a variety of wild and domestic animals. It has a significant impact on the health and welfare of grazing sheep, cattle, and goats, leading to substantial losses in milk, meat production, and fertility. The global economic losses are estimated at \$ 3 billion (1). Additionally, the treatment of infected animals and the implementation of integrated control programs incur considerable costs (2). Furthermore, the impact of Fasciola hepatica extends beyond livestock, posing a significant zoonotic threat. The disease affects 2.4 to 17 million people across more than 70 countries and has been recognized as a neglected foodborne trematode by the WHO (3). This dual impact on both animal agriculture and human health underscores the critical need for advanced and sustainable control strategies.

Since vaccination against fasciolosis is not available, current control measures rely on anthelmintic treatment; however, resistance to fasciolicides, such as triclabendazole or clorsulon, has emerged in some areas (4). Preventing infection through vaccination would be an ideal addition to integrated control methods, helping to reduce parasite loads in herds and potentially circumventing the development of resistance. Fasciola hepatica has evolved mechanisms that skew the host immune response towards non-protective Th2 and regulatory Treg profiles while suppressing Th1 and cytotoxic immunity (5). In both rodent models and natural ruminant hosts, infection initially triggers a mixed Th1/Th2 response (with increases in IFN- γ , IL-4, IL-10, and TGF- β). Eventually, a dominant Th2/Treg environment quickly develops, characterized by high levels of IL-4 and IL-10, alternative macrophage activation (6, 7), and the expansion of IL-10producing Tregs (8). At the same time, pro-inflammatory Th1 cytokines (e.g., IFN-γ) and cytotoxic CD8+ T cell responses are suppressed, resulting in weak IgG1/IgG2a antibody production and ineffective cell-mediated killing, which enables the parasite to establish chronic infections (9).

Over the past few decades, several antigens have been investigated as vaccine candidates, among which glutathione Stransferases (GST), cathepsin L proteases (CL), leucine

aminopeptidases (LAP), and fatty-acid-binding proteins (FABP) stand out as leading targets (10-14). FABPs are molecules synthesized by the parasite to sequester essential fatty acids from the host since trematodes cannot synthesize long-chain lipids (15). These proteins have already been used as vaccination candidates through various technologies, providing partial protection against Fasciola hepatica (10, 16, 17) or Schistosoma mansoni (18). Among these, recombinant Fh15, a Fasciola hepatica FABP, has shown significant potential, inducing partial protective immunity in mice and sheep models (19). Furthermore, Fh15 has been shown to modulate the host's immune response by reducing inflammation and suppressing lipopolysaccharide (LPS)-induced cytokine storm (20). Despite these promising findings and the significant efforts in classical vaccine development, no vaccine has yet achieved complete protection or been approved for commercial use; therefore, fasciolosis remains without an effective immunoprophylactic solution. In recent years, mRNA technology has emerged as a promising strategy for vaccination that could be effective against parasites (21). Early studies on helminths have shown that it can be an effective method to elicit immunity using parasite proteins (22). Thus, this technology may be developed to express Fasciola hepatica proteins and elicit an immune response against the parasite. Our study aims to evaluate the immunogenic potential of the FABP Fh15 produced by an optimized mRNA construct and formulated in lipidic nanoparticles for in vivo testing.

2 Materials and methods

2.1 Animal handling

Animal procedures were conducted under Spanish (RD 53/2013) and European Union (Directive 2010/63/CE) regulations regarding animal experimentation. The accredited Animal Experimentation Facilities (Registration number: PAE/SA/001) of the University of Salamanca (USAL) were used for such procedures. Animals were maintained in standard polycarbonate and wire cages, with controlled 12-hour light and dark periods, a temperature of 23-25°C, and food and water available *ad libitum*.

The USAL's Research Ethics Committee approved the procedures used in this study (Ref. CEI 1057). Every effort was made to minimize animal suffering.

2.2 mRNA design and cloning

The sequence of the FABP Fh15 was retrieved from UniProt (Q7M4G0), reverse-translated, and codon-optimized using the GenSmart Codon Optimization tool for human and mouse expression hosts. Optimized sequences were synthesized using GenTitan Gene fragment and cloned into our previously described mRNA expression vector (23) by restriction cloning. Briefly, this vector was designed by placing in a pUC57mini backbone the CleanCap AG-adapted T7 RNA polymerase promoter upstream of the human alpha-globin 5' UTR (24), the 3' UTR AES-mtRNR1, which confers increased transcript stability (25), and a segmented 100-nt poly(A) tail interrupted by a short linker (A30LA70, where L = GCAUAUGACU) (26), followed by a BspQI restriction site.

2.3 mRNA transcription

Plasmid DNA was linearized using the BspQI restriction enzyme (R0712S, NEB, Ipswich, MA, USA) by 16-hour digestion followed by phenol-chloroform extraction. Next, 1 μg of linearized plasmid was used as a template for *in vitro* transcription (IVT) using the HiScribe[®] T7 Quick High Yield RNA Synthesis Kit (E2050S, NEB, Ipswich, MA, USA), incubation for 16 hours at 37°C with 4 mM CleanCap AG (TriLink Biotechnologies, San Diego, CA, USA).

In vitro transcribed mRNA (FABP-mRNA) was treated with DNase I (M0303, NEB, Ipswich, MA, USA) to remove the template and then precipitated by adding LiCl to a final concentration of 2.5 M, incubating for 1h at −20°C, and centrifuging for 30 min at maximum speed. Then, the pellet was washed twice with 70% ethanol. The mRNAs were resuspended in nuclease-free water and quantified using A260/A280 spectroscopy in a NanoDrop 2000 (Thermo Scientific, Waltham, MA, USA).

Subsequently, dsRNA was removed by cellulose purification (27). Briefly, 500 μg of mRNA in chromatography buffer (10 mM HEPES, 0.1 mM EDTA, 125 mM NaCl & 16% EtOH) was added to a NucleoSpin filter column (740606, Machery-Nagel) preloaded with 0.14 μg cellulose (C6288, Sigma-Aldrich). The column was shaken for 30 minutes and then centrifuged for 60 seconds at 14,000 g to collect the eluate. The eluate was precipitated with 0.1 volume of 3 M NaOAc and 1 volume of isopropanol, washed with 70% ethanol, and resuspended in nuclease-free water.

2.4 mRNA in vitro transfection

The protein production of the FABP mRNA was assessed by transfecting HEK293T cells (ATCC) cultured in DMEM (10569010,

Gibco, Thermo Scientific, Waltham, MA, USA) 10% FBS (A5209502, Gibco, Thermo Scientific, Waltham, MA, USA), at 37°C with 5% CO2. Briefly, 24-well plates at 70% confluence were transfected with 10 μ g of purified mRNA using 1 μ L of Lipofectamine MessengerMax (LMRNA003, Invitrogen, Waltham, MA, USA) per well, according to the manufacturer's protocol, and then incubated for 24 h. To harvest, the cells were lysed in 1x RIPA buffer (9806S, Cell Signaling Technologies, Danvers, MA, USA) with protease inhibitors (5871, Cell Signaling Technologies, Danvers, MA, USA). Cell lysates were centrifuged at maximum speed for 10 minutes, and the protein concentration in the clarified supernatant was quantified using the Pierce BCA protein assay kit (23225, Thermo Scientific, Waltham, MA, USA) and analyzed by SDS-PAGE.

2.5 Western blot

SDS-PAGE was used to verify protein expression in HEK-293T cells and to assess IgG presence against recombinant Fh15 (rFH15) in mouse serum. Briefly, 30 µg of lysate or the rFh15 were boiled at 95°C for 10 min in 1X SDS-PAGE Sample Loading Buffer (MB11701, NZYTech, Lisboa, Portugal) supplemented with βmercaptoethanol. The boiled protein was separated by SDS-PAGE using precast gradient gels (MB46601, NZYTech, Lisboa, Portugal) and transferred to nitrocellulose membranes (88018, Thermo Scientific, Waltham, MA, USA). Following transfer, membranes were blocked for 60 min in 5% skimmed milk and subsequently incubated overnight at 4°C with either a 1:1000 dilution of anti-HisTag (MA121315, Invitrogen, Waltham, MA, USA) or mouse serum diluted 1:500 in 5% skimmed milk. After incubation, membranes were washed three times for 10 minutes each in 1x PBST (0.1% Tween 20). Membranes were incubated for 60 min with anti-mouse IgG-HRP secondary antibody (A9044, Sigma-Aldrich, St. Louis, MO, USA) diluted 1:10,000 in 5% skim milk in PBS. After secondary antibody incubation, membranes were washed three times for 10 minutes each in 1x PBST. Lastly, the membranes were developed by incubating for 3 min with NZY Advanced ECL (MB40201, NZYTech, Lisboa, Portugal), imaged using a ChemiDoc (Bio-Rad, Hercules, CA, USA).

2.6 Murine immunization

mRNA was encapsulated using a microfluidic chip through GeneScript's custom mRNA LNP service, which employed SM102 (28) as the ionizable lipid.

Twelve 11-week-old BALB/c female mice were randomly divided into two groups (n=6) and immunized using a prime-boost scheme (Figure 1A), with a 21-day interval between immunizations. Immunization was performed intramuscularly on the gastrocnemius with a 30-gauge syringe. One group received 15 μ g LNP-encapsulated mRNA while the other received equivalent amounts of empty LNP with each dose. Blood samples were collected longitudinally at four time points: pre-immunization, 24

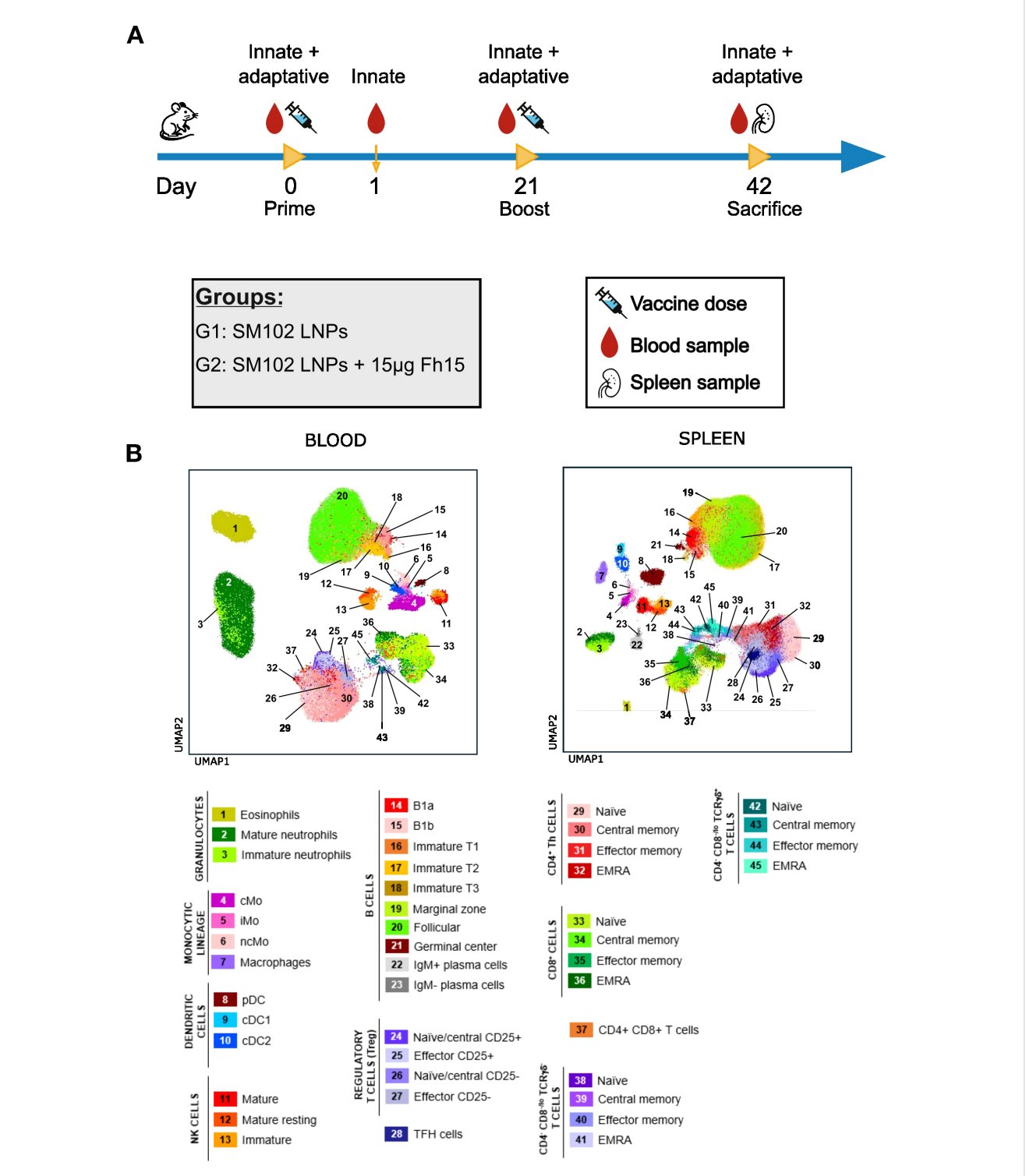


FIGURE 1 Experimental design and immune landscape of blood and spleen samples. (A) Schematic representation of the immunization schedule and sample collection. Mice were primed on day 0 and boosted on day 21 with SM102 LNPs (G1) or SM102 LNPs encapsulating 15 µg FABP mRNA (G2). Peripheral blood was collected at days 0, 1, 21, and 42, and spleens were collected at necropsy (day 42). (B) UMAP plots show the immune cell landscape in peripheral blood (left) and spleen (right) based on flow cytometry data. cMo, classical monocytes; iMo, intermediate monocytes; ncMo, non-classical monocytes; pDC, plasmacytoid dendritic cell; cDC, conventional dendritic cell; Th, T helper; TFH, T follicular helper cell; TCR, T cell receptor; NK, natural killer.

hours after the first dose, just before the second dose, and 21 days after the second dose. Spleens were collected after sacrifice at the end of the experiment and disaggregated using 0.40 μm cell strainers. Posterior analysis was performed blinded to group and mouse distribution.

2.7 Immunophenotypic studies

Ex vivo characterization of blood and spleen immune cells (Figure 1B) was performed using 50 µL of EDTA-anticoagulated, plasma-depleted blood and 2 \times 10⁶ cells from spleen cell suspensions. Spleen suspensions were prepared by homogenizing spleens in PBS with a 21G syringe, followed by filtration through a 70 μm cell strainer. All samples were stained employing a stain-lysewash procedure. Blood samples were multiplexed (2 samples per tube) using a barcoding strategy with distinct fluorochromeconjugated CD45 antibodies (Supplementary Table 1). Individual blood and spleen samples were first washed with PBS, pH 7.4 for 5 minutes at 540 x g. Samples were then pre-incubated for 30 minutes at room temperature (RT), protected from light, with the distinct barcoding antibodies (blood samples only), anti-CD3 antibody (blood and spleen samples), True-Stain Monocyte Blocker (Biolegend, San Diego, CA), TruStain FcXTM PLUS (Biolegend), and Zombie NIR viability marker (Biolegend, 1:2000 dilution). Following the pre-incubation, blood samples were washed with PBS containing 0.5% bovine serum albumin (BSA), 0.1% sodium azide, and 2 mM EDTA (pH 7.4). Samples to be multiplexed were then combined into a single tube. The remaining panel of antibodies (detailed in Supplementary Table 1) and Brilliant Staining Buffer Plus (BD Biosciences, San Jose, CA) were added, and samples incubated for 30 minutes at RT, protected from light, on a roller. To lyse red blood cells and fix the samples, 1X BD FACS Lysing Solution (BD Biosciences) was added and incubated for 10 minutes at RT, protected from light. Samples were subsequently washed with PBS containing 0.5% BSA, 0.1% sodium azide, and 2 mM EDTA (pH 7.4) (540 xg for 5 min), and resuspended in 400 μL of PBS before flow cytometry analysis.

2.8 Splenocyte culture and immunostaining

Spleens were homogenized in PBS using a 21G syringe and filtered through a 70 μm cell strainer to prepare single-cell suspensions. Splenocytes were seeded at a density of 1 x10 6 cells/ mL in 24-well plates containing 500 μL of RPMI supplemented with 2 mM L-glutamine, 1% penicillin-streptomycin, and 10% FBS for 24 hours at 37°C with 5% CO2. After this initial incubation, the cells were stimulated for 72 hours with either 10 $\mu g/mL$ of recombinant Fh15 (rFh15) or 2.5 $\mu g/mL$ of Phytohemagglutinin (PHA). Following incubation, cells were centrifuged (540×g for 5 min), and the supernatant was removed. Cells were then washed once with PBS containing 0.5% BSA, 0.1% sodium azide, and 2 mM

EDTA (pH 7.4). Samples were multiplexed (3 samples per tube) using a barcoding strategy with distinct fluorochrome-conjugated CD45 antibodies (Supplementary Table 1). Samples were preincubated for 30 minutes at RT, protected from light, with the barcoding antibodies, True-Stain Monocyte Blocker (BioLegend), TruStain FcXTM PLUS (BioLegend), and Zombie NIR viability marker (BioLegend, 1:2000 dilution). After pre-incubation, samples were washed with PBS containing 0.5% BSA, 0.1% sodium azide, and 2 mM EDTA (pH 7.4) and combined into a single tube. Cells were then incubated with surface antibodies (Supplementary Table 1) for 30 minutes at RT in the dark, then fixed and permeabilized using the eBioscience TM Foxp3 Transcription Factor Staining Buffer Set (ThermoFisher Scientific, 00-5523-00) following the manufacturer's instructions. Briefly, 1 mL of freshly prepared 1X Fixation/Permeabilization Buffer was added, and samples were incubated for 30 minutes at room temperature. After washing twice with 2 mL of 1X Permeabilization Buffer (centrifugation at 540×g for 5 min), the cells were resuspended in 100 µL of 1X Permeabilization Buffer containing intracellular antibodies (Supplementary Table 1) and incubated for 30 minutes at RT in the dark. Cells were then washed twice with 2 mL of 1X Permeabilization Buffer, resuspended in 300 µL of PBS, and analyzed immediately or stored at 4°C for up to 1 hour before acquisition.

2.9 Flow cytometry data acquisition and analysis

Data acquisition was performed on an Aurora spectral flow cytometer (Cytek, Fremont, CA) equipped with five lasers (355 nm, 405 nm, 488 nm, 561 nm, 640 nm). Daily instrument setup and quality control were performed using SpectroFlo QC beads (Cytek) according to the manufacturer's instructions before sample measurement. To ensure accurate spectral unmixing, single-stained reference controls for each fluorochrome in the antibody panel, along with an unstained control sample, were processed identically to the multicolor-stained samples (Supplementary Table 2). The resulting unmixing matrix was generated using SpectroFlo software (v3.3.0; Cytek). The accuracy of the unmixing was assessed by comparing its performance with single-stained references and the full-stained sample using NxN plots.

Data analysis was conducted using InfinicytTM software (version 2.1.0.a.000; BD Biosciences). For flow cytometric data analysis, initial gating excluded dead cells based on Zombie NIR live/dead marker expression and a parameter ν s. time plot was employed to exclude events exhibiting unstable acquisition signal fluctuation (e.g. due to start-up/end of acquisition or clogs). Subsequently, doublets were removed by gating on forward scatter area (FSC-A) versus forward scatter height (FSC-H). Non-lysed red blood cells were excluded from the analysis using the side scatter (SSC) signal from both the blue and violet lasers. Leukocytes were defined as CD45-positive cells. Specific immune cell populations were identified based on their immunophenotypic profiles, as detailed in Supplementary Table 3

and Supplementary Figure 1. T cell maturation was determined by the expression of CD27, CD44, and CD62L. Accordingly, naïve cells were defined as CD27+ CD44- CD62L+, central plus effector memory (CM+EM) as CD44+, and effector memory re-expressing CD45RA (EMRA) as CD27- CD62L- CD44-/lo). All flow cytometric data analysis was performed with Infinicyt software version 2.1.0.a (BD Biosciences, San Jose, CA, USA). Unmixed.fcs files are available at the University of Salamanca Gredos repository (http://hdl.handle.net/10366/167455).

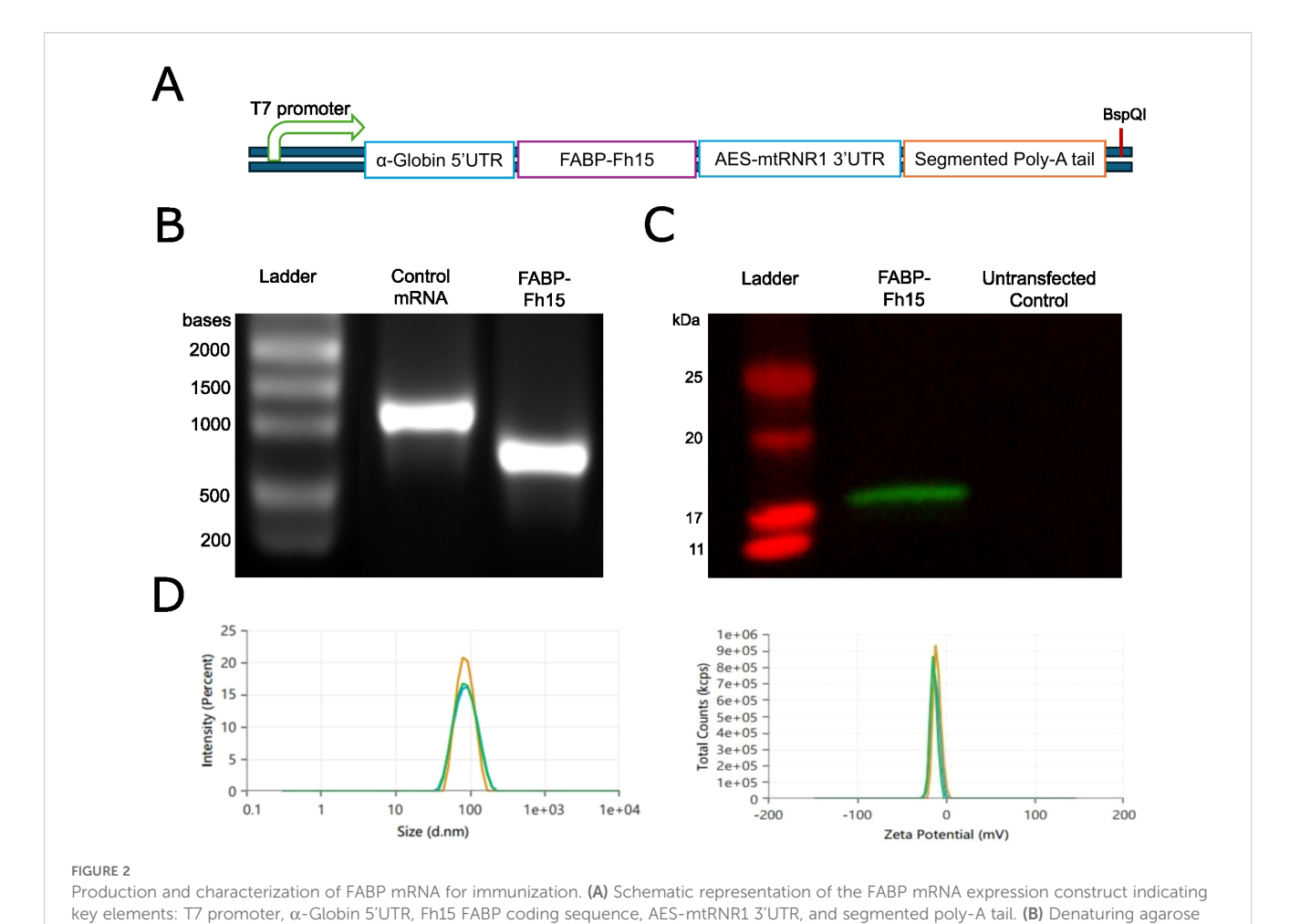
2.10 Data analysis

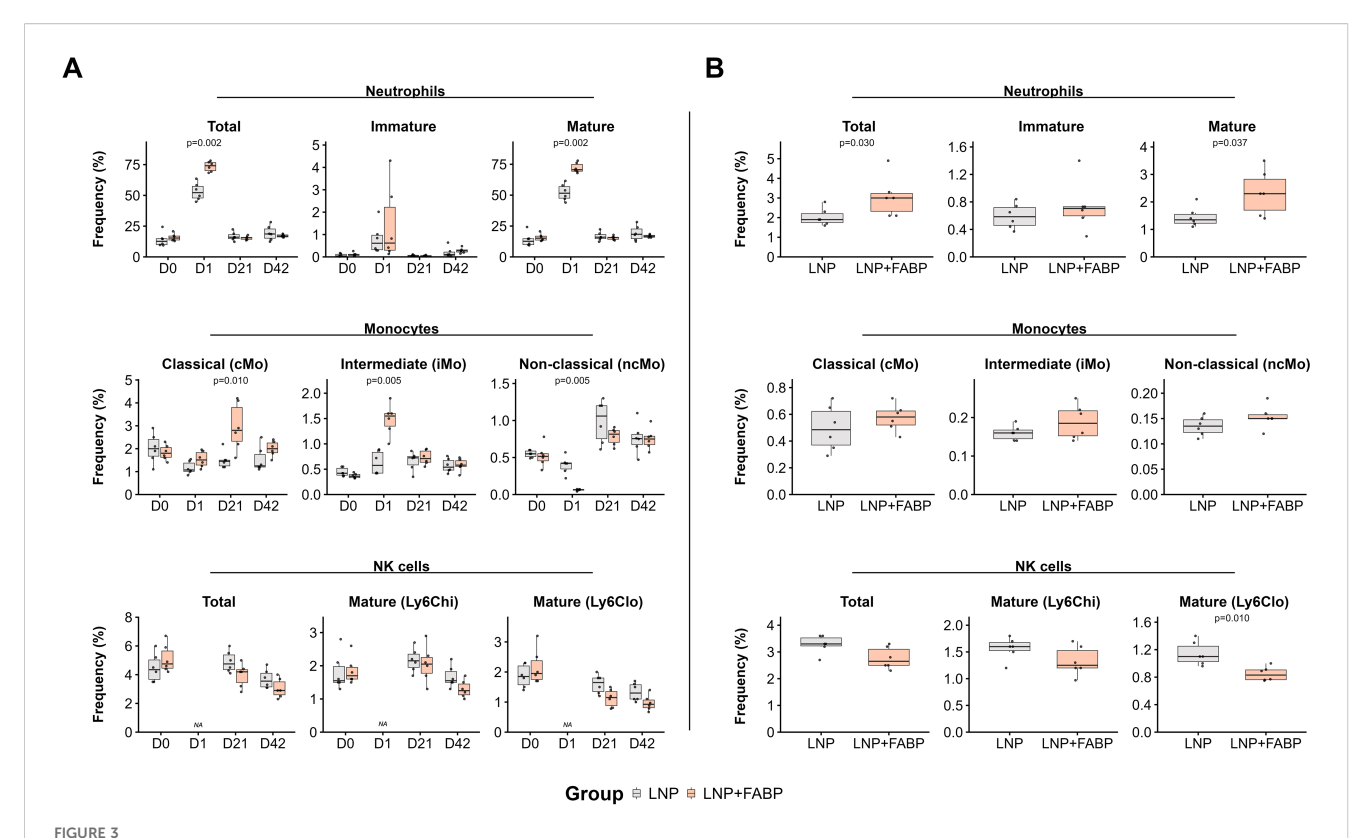
All data were analyzed by using the R environment (29). Figures were plotted using the "ggplot2" package (30). Comparisons were made by the Wilcoxon rank sum test and exact p-values were shown. The Benjamin-Hochberg method was applied to control for the False Discovery Rate (FDR). Findings were considered statistically significant if the FDR q-value was <0.05. R files are available on Git-Hub (https://github.com/Sanchez-Montejo/Manuscript-Fh15).

3 Results

3.1 mRNA expression of F. hepatica FABP

We optimized the sequence of F. hepatica FABP Fh15 for expression in human and mouse cells, subsequently cloning it into our mRNA expression vector (Figure 2A). We performed in vitro transcription (IVT) with co-transcriptional capping and removed any possible dsRNA contamination using cellulosepacked columns. We then analyzed the transcription product using denaturing agarose gel electrophoresis to observe a noticeable band of the expected size (Figure 2B). Finally, we transfected the purified transcripts into HEK293T cells and analyzed protein production via western blotting (WB) with an anti-histidine antibody. The WB showed a band corresponding to the estimated size of the cloned FABP (Figure 2C). The capped mRNA was encapsulated into SM102 LNPs by GeneScript. The characteristics of the final particles were assessed to ensure proper mRNA encapsulation efficiency (91.65%), Z-potential (-10.2100 mV), average particle size (82.43 nm), and polydispersity index (0.08) (Figure 2D).





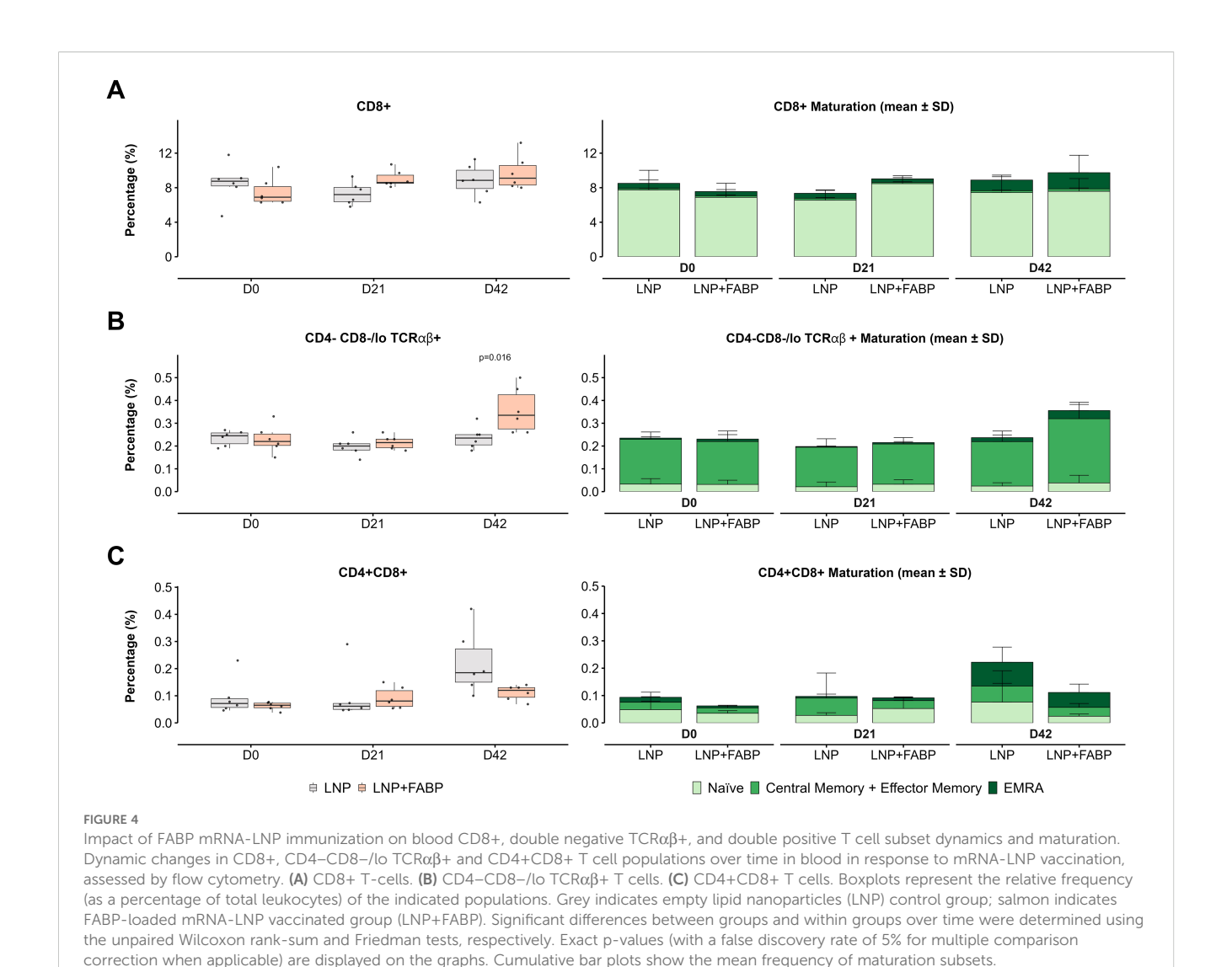
Impact of FABP mRNA-LNP vaccination on innate immune cell populations. Modulation of innate cell populations in blood and spleen in response to mRNA-LNP vaccination, as assessed by flow cytometry. (A) Relative frequency of neutrophil, monocytes, and NK cells, reported as percentage from total leukocytes, longitudinally evaluated in peripheral blood at different time points. (B) Relative frequency of neutrophils, monocytes, and NK cells, as a percentage of total leukocytes, in spleen samples after necropsy. Boxplots represent the frequency (%) of neutrophils (total, immature, mature subsets), monocytes (classical [cMo], intermediate [iMo], non-classical [ncMo] subsets), and natural killer (NK) cells (total, mature Ly6Ch¹, mature Ly6Clo subsets). Grey indicates the empty lipid nanoparticles (LNP) control group, and salmon indicates the FABP-loaded mRNA-LNP vaccinated group (LNP+FABP). Significant differences were determined using the unpaired Wilcoxon rank-sum test; exact p-values are displayed on the graphs.

3.2 Mice immunized with FABP mRNA-LNP show an enhanced innate immune response

Mice immunized with either LNPs or the FABP mRNA encapsulated in LNP exhibited some degree of innate immune response (Figure 3). Accordingly, one day post-immunization, a significant increase in total neutrophil counts was observed in peripheral blood. This increase, reflecting a higher frequency of both mature and immature neutrophils, was observed in mice receiving either empty LNP or FABP mRNA-LNP. However, this effect was significantly more pronounced in mice immunized with the FABP mRNA vaccine, particularly for mature neutrophils (p=0.02; Figure 3A). A similar increase in the frequency of mature neutrophils was also observed in spleen samples from the mRNA group (Figure 3B). Conversely, significant sequential cellular kinetics in monocytic populations in blood were only observed in mice immunized with the LNP-encapsulated FABP mRNA. Specifically, at D1 post-immunization, non-classical monocytes (ncMo) transiently declined, suggesting their mobilization to the tissue, while a notable surge in intermediate monocytes (iMo) occurred concurrently. By 21 days postimmunization, the frequency of circulating classical monocytes (cMo) had increased significantly, likely reflecting a compensatory response and new production in the bone marrow. Interestingly, while clear kinetics were observed in blood, no significant differences between the groups were detected in the spleen samples (Figure 3B). Of note, no significant impact of the vaccine was observed for eosinophils, basophils, and dendritic cell populations in both blood and spleen (data not shown). Immunization with LNP-encapsulated FABP mRNA was associated with lower numbers of circulating natural killer (NK) cells, compared to empty LNP, particularly of mature NK cells with an activated/effector profile (Ly6Clo NK cells), both in blood and spleen samples. Overall, while the empty LNP induced some innate responses, mice immunized with the FABP mRNA encapsulated LNP differential innate immune response.

3.3 Immunization with FABP mRNA-LNP induces T-cell antigen-specific responses

Overall, a significant increase in the frequency of total T cells in blood was observed over time in mice immunized with FABP mRNA-LNP (p=0.004 for D0 *vs.* D21 and p=0.02 for D0 *vs.* D42, but not for those receiving empty LNP. In line with this global T cell trend, only

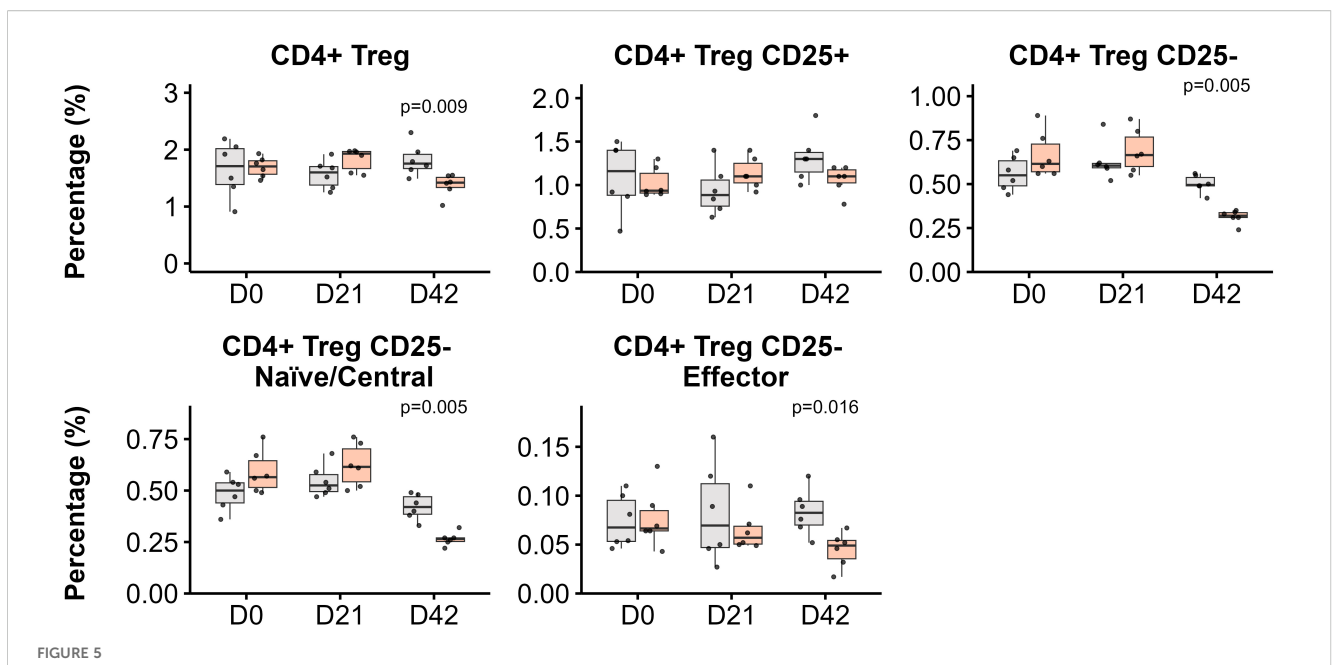


animals immunized with FABP mRNA-LNP displayed an increased frequency of circulating CD8+ T cells in peripheral blood (p=0.01 for D0 vs. D21 and D42; Figure 4A). Furthermore, this increase was primarily driven by effector CD8+ EMRA T-cells. Interestingly, while no significant modulation of CD4-CD8-/lo TCRγδ+ cells was observed (data not shown), CD4-CD8-/lo TCRαβ+ cells (TCRαβ+ DNT cells) exhibited a specific response to the presence of mRNA, post boosting, showing a significant increase on D42 (Figure 4B), with a median cell number that nearly doubled that of the control group and D0 samples. In line with CD8+ T cells, this increased frequency resulted from the expansion of central/effector memory and EMRA populations (Figure 4B). Conversely, CD4+ CD8+ T cells (DPT cells) displayed a trend of increased frequency in blood over time; this expansion was more pronounced in the empty LNP group at D42 (p=0.037 vs. FABP-loaded mRNA-LNP) (Figure 4C). Of note, no significant differences in the frequency of these populations were observed in the spleen (data not shown).

Regulatory T cells (Tregs) also exhibited a specific modulation as a result of immunization with FABP mRNA-LNP in peripheral

blood (Figure 5). This group showed a significant decrease in the frequency of circulating Tregs compared with the LNP-only group post-boosting (p = 0.009). This decline was primarily driven by the peripherally induced CD25- Tregs (p=0.005), with both naïve/central and effector cell populations showing diminished frequencies (Figure 5).

Overall, total CD4+ T-helper (Th) cell frequency in peripheral blood showed minimal modulation after immunization, with only a slight increase observed post-boosting (median 1.3-fold for empty LNP and 1.2-fold for the FABP mRNA-LNP, compared to D0) (Figure 6A). However, analysis of the maturation profile of these cells revealed an increased proportion of memory and effector (CM+EM and EMRA) cells, at the expense of the naïve compartment, particularly in the FABP-loaded mRNA-LNP group (Figure 6B). While no significant differences in overall frequency (Figure 6C) and maturation profiles (Figure 6D) were observed between the groups in the spleen, upon stimulation with rFh15 antigen, splenocytes from mice immunized with FABP-loaded mRNA-LNP exhibited an increased frequency of antigen-



CD4+ regulatory T cell (Tregs) subpopulations in blood post-immunization. Kinetics of Treg populations in response to LNP and FABP-loaded mRNA-LNP, as assessed by flow cytometry. The relative frequencies from total leukocytes of total CD4+ Tregs, along with their CD25+ and CD25-subsets, are shown. Within the CD25- Treg population, both naïve/central and effector cell frequencies are also depicted. Boxplots represent the frequency (%) of indicated populations. Grey indicates empty lipid nanoparticles (LNP) control group; salmon indicates the FABP-loaded mRNA-LNP vaccinated group (LNP+FABP). Significant differences between groups were determined using the unpaired Wilcoxon rank-sum test; exact p-values (with a False Discovery Rate of 5% for multiple comparison correction when applicable) are displayed on the graphs.

specific Th1 and Th2 cells, as assessed by the expression of t-Bet and GATA-3 transcription factors (Figure 6E).

3.4 Immunization with FABP mRNA-LNP induces B-cell responses and antigenspecific antibody production

Overall, while the FABP-loaded mRNA-LNP did not significantly affect B1 cell populations in either blood or spleen (data not shown), a significant impact was observed for different B2-cell subsets. Specifically, a substantially lower frequency of immature B cells was detected in blood and spleen in mice immunized with FABP-loaded mRNA-LNP, compared to those exposed to empty LNP (Figures 7A, B). This reduction in immature forms was concurrently associated with an expansion of the mature B cell compartment in both blood (D21) and spleen, suggesting the induction of B cell maturation following immunization. Interestingly, although exposure to empty LNP also induced B cell kinetics in blood, the FABP-loaded mRNA-LNP group exhibited a faster and more pronounced response. Specifically, while both groups experienced expansions of mature B2 populations, the FABP-loaded mRNA-LNP group transitioned towards mature B-cell subsets after the first dose. In contrast, the empty LNP group required a booster to achieve similar maturation effects (Figure 7A).

Additionally, detailed maturation profile analysis of spleen mature B2 cells revealed that immunization with the FABP

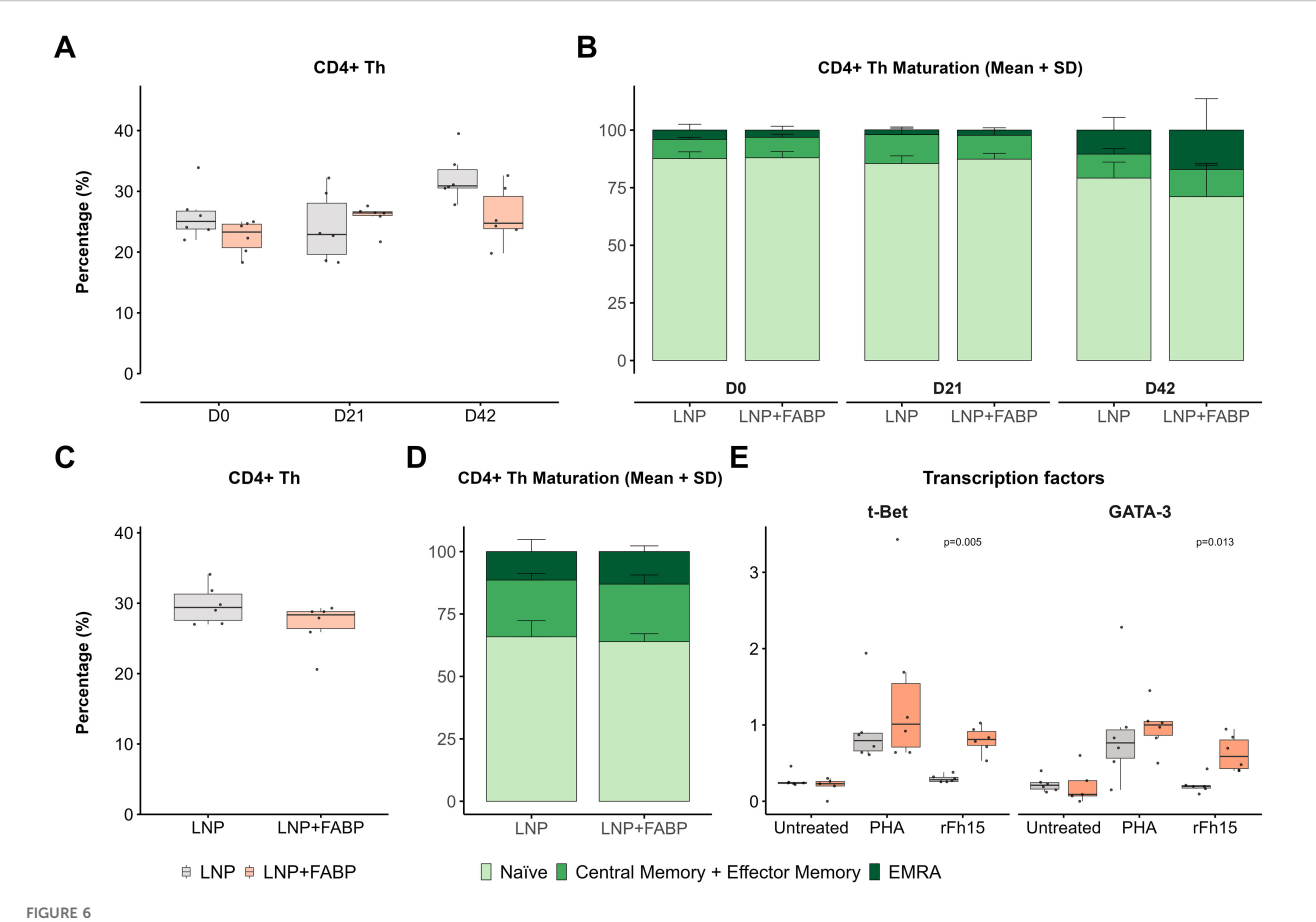
mRNA led to expansion of marginal zone, follicular, and germinal center B cell subsets (Figure 7C), compared to empty LNP.

Finally, the humoral response generated by the immunization was evaluated. Interestingly, despite no significant differences in plasma cell frequency being observed in the spleen post-boosting (Figure 8A), the frequency of class-switched (IgM⁻) plasma cells was significantly higher in mice immunized with the FABP-loaded mRNA-LNP. This was further corroborated by the detection of IgG antibodies recognizing the recombinant protein rFh15 in plasma by Western Blot (Figure 8B), which was observed exclusively in the mRNA-vaccinated group.

4 Discussion

The primary aim of this study was to develop and characterize an mRNA-based vaccine using the FABP protein (Fh15) of *Fasciola hepatica*, a primary causative agent of fasciolosis. In this study, we optimized the sequence of the FABP Fh15 and cloned it into an mRNA vector, which was then expressed *in vitro* using the HEK293T cell line and encapsulated in LNPs for mouse immunization.

Mice immunized with FABP mRNA-LNP exhibited rapid innate immune activation, with early mobilization and maturation of neutrophils. As expected during acute inflammation, immature neutrophils increased in circulation, compensating for tissue migration ("left shift") (31). This is consistent with local inflammation induced by mRNA LNP-based vaccines, where local inflammation is induced at the injection site



CD4+ helper T-cells (Th) after FABP mRNA-LNP immunization. Modulation of CD4+ T-helper cell populations and their antigen-specific responses following FABP mRNA-LNP immunization, as assessed by flow cytometry. (A) Longitudinal kinetics and maturation profile of CD4+ Th cells in peripheral blood post-immunization. Boxplots represent their frequency within total leukocytes. (B) Stacked bars (right) depict the relative distribution of the different maturation stages (naïve, central/effector memory, EMRA) within CD4+ Th cells. (C) CD4+ T-helper cell analysis in the spleen at necropsy. Boxplots show frequency within total leukocytes. (D) Stacked bars show maturation profile within the CD4+ Th population in spleen. (E) Frequency of Th1 and Th2 responses in spleen, assessed by the expression of transcription factors t-Bet and GATA-3 after *in vitro* stimulation with PHA or recombinant Fh15 protein (rFh15). Grey indicates empty lipid nanoparticles (LNP) control group; salmon indicates FABP-loaded mRNA-LNP vaccinated group (LNP+FABP). Significant differences between groups were assessed using the unpaired Wilcoxon rank-sum test; exact p-values (with a False Discovery Rate of 5% for multiple comparison correction when applicable) are displayed on the graphs.

due to the presence of the LNPs (32) and the presence of unmodified mRNA (33). In contrast, monocyte responses were specific to FABP mRNA-LNP. At 24 h post-immunization, patrolling ncMo were depleted, suggesting migration to inflamed tissues (34). This decrease in ncMo at D1 was associated with a nearly 3-fold increase in circulating iMo. Notably, while mouse iMo are less characterized, the intermediate CD14+/CD16+ monocyte subset is characterized by high surface expression of antigenpresenting and co-stimulatory molecules, including HLA-DR, CD80, and CD86 (35). Our observation of increased intermediate monocytes (with presumably higher MHC-II, CD80, and CD86 expression) in the FABP-immunized group suggests ongoing antigen immune activation, consistent with prior reports that intermediate monocytes upregulate these markers during infection or immunization (36). Furthermore, the rise in circulating iMo aligns with an inflammatory response, as has been documented in various human disease conditions, including malaria (37). Interestingly, despite clear monocyte kinetics being observed in blood specifically in response to FABP-loaded mRNA- LNP immunization, no significant differences were observed in the spleen for these populations. The spleen is a critical reservoir for monocytes, providing a large and rapidly deployable pool that complements the continuous surveillance and initial response of blood monocytes. This splenic reserve is crucial for combating larger infections and managing significant inflammatory events (38). Therefore, the lack of kinetics observed in spleen monocytic populations suggests that the local inflammation, induced by the vaccine inoculation, was limited, not requiring the deployment of the spleen reservoir. Overall, the additive effect on neutrophils and specific modulation patterns of monocytes suggest that, upon inoculation, the FABP is rapidly produced (within 24 hours) and is immunogenic, capable of triggering an inflammatory response that remains immunologically controlled, thereby avoiding extreme inflammation, a significant safety concern for vaccine development. However, the lack of a mock mRNA in the control group difficulties the discrimination of the specific effect of the FABP versus an irrelevant mRNA. Additionally, we observed a decrease in circulating mature NK cells, particularly those with activated/

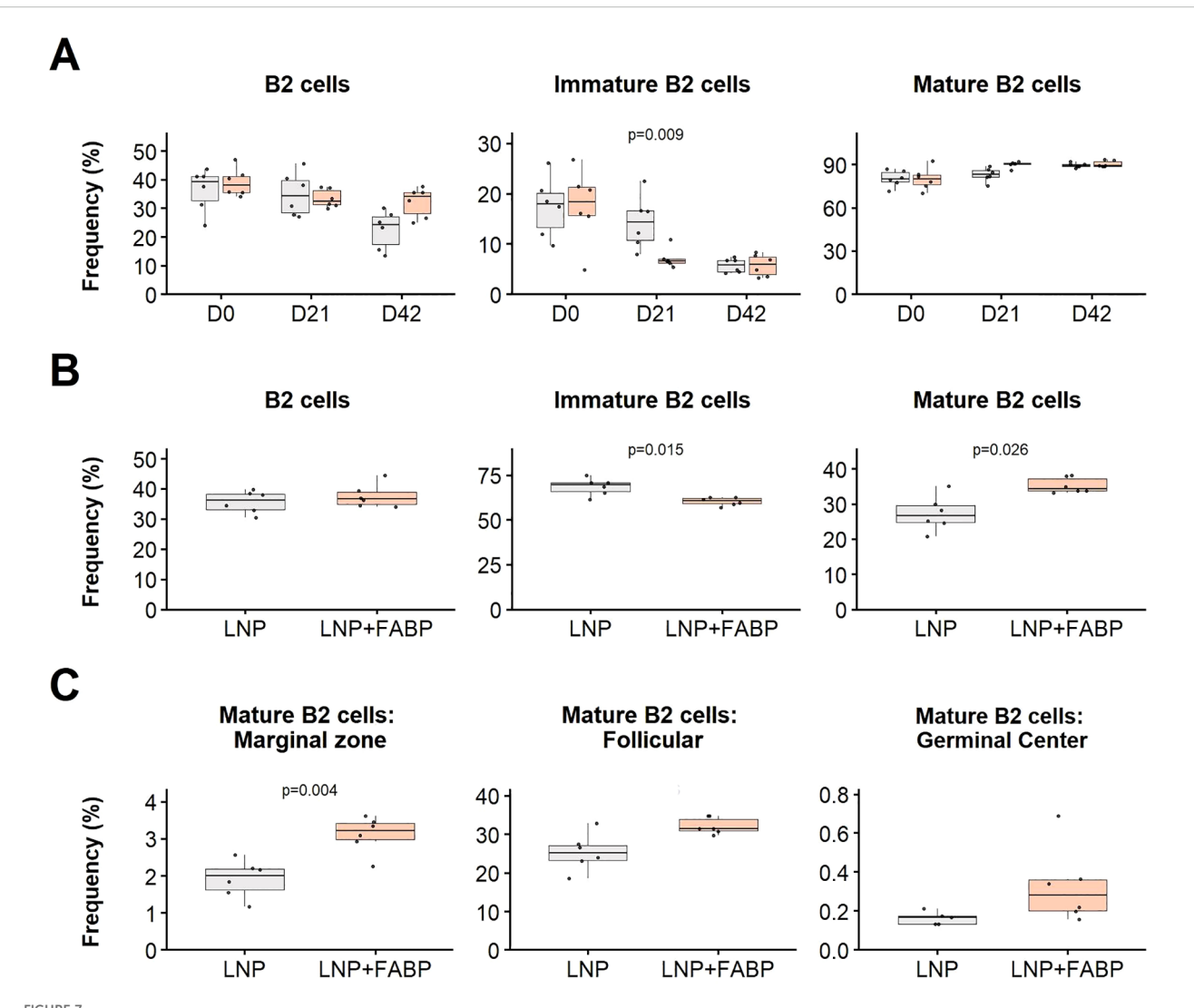
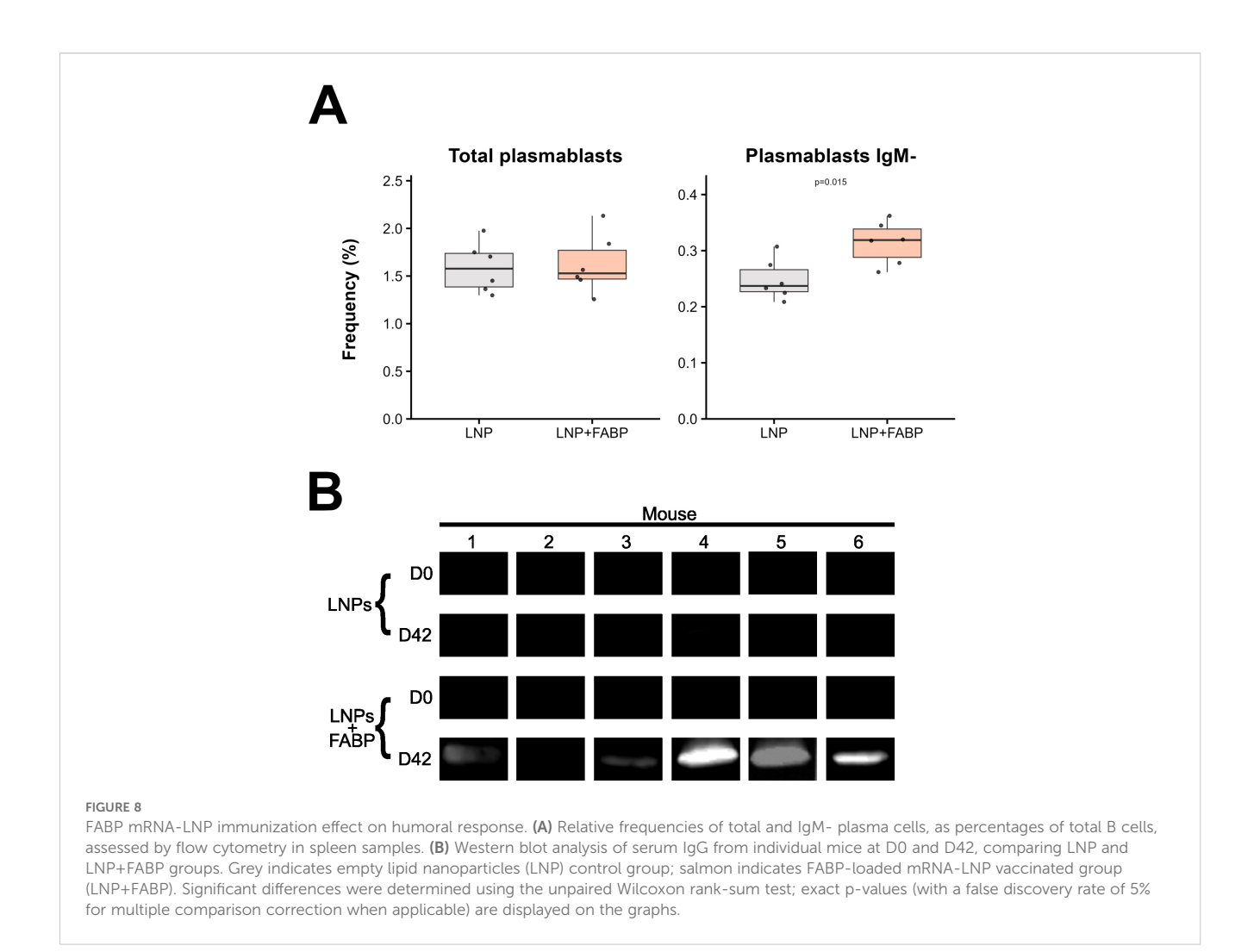


FIGURE 7

Effect of FABP mRNA-LNP immunization on B cell populations. Modulation of B2 cell subsets in blood and spleen in response to mRNA-LNP vaccination, as assessed by flow cytometry. (A) Relative frequency of major B2 cell subpopulations in peripheral blood at different time points post-immunization. Boxplots represent the frequency (%) of total, immature, and mature B2 cells within total leukocytes. (B) Relative frequency of B2 cells in the spleen at necropsy. Frequencies (%) of total, immature, and mature B2 cells are shown relative to total leukocytes. (C) Maturation profile of splenic mature B2 cells: marginal zone, follicular, and germinal center. Frequencies are expressed as a proportion of total B2 cells. Grey indicates empty lipid nanoparticles (LNP) control group; salmon indicates FABP-loaded mRNA-LNP vaccinated group (LNP+FABP). Significant differences between groups were determined using the unpaired Wilcoxon rank-sum test; Exact p-values (with a false discovery rate of 5% for multiple comparison correction when applicable) are displayed on the graphs.

effector functions (Ly6Clo), after each dose. This reduction would be consistent with the recruitment of these cells to lymphoid organs (e.g., draining lymph nodes) upon activation (39), although this should be properly confirmed by analyzing in a new vaccination experiment. Similar findings have been reported with other mRNA vaccines, where activated NK cells and other lymphocytes traffic to lymph nodes as part of the vaccine response, as it induces the recruitment of IL6+ dendritic cells and promotes the B cell response (40). In this study, we did not find significant differences in the relative frequency of dendritic cells in the peripheral blood or spleen, likely due to their accumulation in draining lymph nodes or the injection site (32). This should be specifically addressed by studying lymph node populations in future studies.

Evaluation of cellular immune responses following immunization with the FABP mRNA-LNP formulation showed a significant increase in TCR $\alpha\beta$ + DN T-cell populations, especially within the effector (EMRA) subset, known to promote Th1, Th2, and Th17 responses and to be key in immunity against parasites like Leishmania spp. (41, 42). In contrast, while double-positive CD4 +CD8+ T cells were significantly increased at D42 in the group immunized with empty LNP, a lower frequency of these cells was observed for the mice exposed to the complete vaccine. Since there was no overall decrease in circulating DP T cells in the complete vaccine group, but rather a shift toward a memory/effector phenotype, this lower frequency likely indicates their potential migration to tissues. DP T cells were antigen-reactive



lymphocytes in the self-cure of *Schistosoma* infections in rhesus macaques (43). This suggests that they could also produce antigen recognition against *Fasciola*, contributing to protective immunity.

LNPs serve as the primary adjuvants for T helper cell stimulation in mRNA immunization (44). In line with this, both study groups exhibited a minor relative frequency increase over time, more pronounced in the control group. Interestingly, despite minor overall differences between groups, which were modest by day 42, significantly different maturation profiles were observed compared to day 0. Both groups showed higher proportions of memory and effector cells, with more pronounced changes in the mRNA group. This pattern suggests that after the booster dose, antigen-specific CD4+ T cells may have migrated to peripheral sites to aid B cell responses. Although no significant differences in total CD4+ T cell frequencies were observed in the spleen, a significantly increased frequency of antigen-specific Th1 and Th2 cells was detected exclusively in the group immunized with FABP-loaded mRNA-LNP. The induction of both responses might help fight the parasite, as Fasciola represses Th1 responses and induces Th2 responses (45). While functional assays, including intracellular cytokine staining/ELIspot and cytotoxicity assays, would provide a definitive measure of immediate T-cell effector function, their inclusion in this study was feasible due to severe limitations in splenocyte availability and the imperative to adhere to the 3R principle of Reduction in animal use. Our decision prioritized T-bet and GATA-3 staining at the 72h time point, which provides a robust measure of vaccine-induced Th1/Th2 lineage commitment and clonal expansion, the central aim of our T-cell analysis.

Finally, we demonstrated that our FABP mRNA induced a humoral response, specifically in the mice that received the mRNA. While both experimental groups showed a significant decrease in immature B2 cells and an increase in mature B2 cells in peripheral blood post-boosting, the timing of these responses differed notably between groups. Mice receiving the mRNA showed a rapid B2 cell kinetic immediately after the first dose, whereas the control group reached similar levels only after the second dose. The lack of significant differences between groups after the second dose, associated with the comparable levels of total plasma cells in the spleen, suggests that the lipid nanoparticle vehicle alone may also trigger some B cell immune response, potentially T-cell independent (46). In line with this, expansion of mature B2 cells in the spleen in mice immunized with FABP-loaded mRNA-LNP reflected the significant increase in the relative frequency of follicular, marginal zone, and germinal center B2 cells. This occurred at the expense of immature cells, ultimately indicating vaccine-induced B cell maturation. Interestingly, despite no

significant differences being observed in the frequency of plasma cells in the spleen between the two groups, mice exposed to the complete vaccine displayed significantly higher frequency of class-switched, IgG-producing plasma cells. This IgG production aligned with the positive detection of the target antigen by western blot, supporting the specificity of the humoral response generated by our mRNA and suggesting that the two-dose FABP-loaded mRNA-LNP vaccination scheme successfully elicited robust antigen-specific primary and class-switched secondary immune responses. These results are similar to those of other mRNA vaccines, which enhance antigen-specific responses and stimulate the activation of germinal centers, ultimately leading to the production of neutralizing antibodies against viruses (47). Notably, the mRNA immunization of *Necator americanus* proteins produced similar maturation of T cells and antigen-specific antibody production (22).

Despite the extensive scientific efforts over the past decades to develop an effective vaccine against *Fasciola hepatica*, the results have been inconsistent and have not led to a satisfactory vaccine (48). Our results demonstrate that the evaluated mRNA can effectively produce a *Fasciola hepatica* protein *in vivo* and induce an immune response that produces both humoral and cellular responses. Further experiments are needed to test this mRNA vaccine against parasite infection, testing whether the effect of the described immune response provides protection against the parasite. However, these experiments have established a foundation for developing an effective mRNA vaccine against *Fasciola hepatica*.

Data availability statement

The original contributions presented in the study are included in the article/Supplementary Material the dataset and data management are available at the GREDOS repository at the University of Salamanca (DOI:10.71636/zmp6-m645) in http://hdl.handle.net/10366/167455. Data management is available on GitHub (https://github.com/Sanchez-Montejo/Manuscript-Fh15). Further inquiries can be directed to the corresponding author/s.

Ethics statement

The animal study was approved by Comité de Ética de la Investigación de la Universidad de Salamanca. The study was conducted in accordance with the local legislation and institutional requirements.

Author contributions

JS-M: Conceptualization, Data curation, Formal Analysis, Investigation, Methodology, Software, Validation, Visualization, Writing – original draft, Writing – review & editing. CT: Conceptualization, Data curation, Formal Analysis, Investigation, Methodology, Validation, Writing – original draft, Writing – review & editing. TS: Data curation, Investigation, Methodology,

Supervision, Validation, Writing - review & editing. JL-A: Conceptualization, Data curation, Investigation, Methodology, Supervision, Writing - original draft. RM-R: Conceptualization, Funding acquisition, Investigation, Methodology, Project administration, Resources, Writing - review & editing. JP: Conceptualization, Data curation, Formal Analysis, Investigation, Validation, Writing - original draft. SM: Formal Analysis, Investigation, Methodology, Writing - review & editing. LS: Investigation, Methodology, Validation, Writing - review & editing. IT: Formal Analysis, Investigation, Methodology, Writing - review & editing. MG-B: Conceptualization, Formal Analysis, Funding acquisition, Project administration, Supervision, Visualization, Writing - original draft, Writing - review & editing. BV: Conceptualization, Formal Analysis, Funding acquisition, Project administration, Resources, Supervision, Validation, Visualization, Writing - original draft, Writing - review & editing. AM: Conceptualization, Formal Analysis, Funding acquisition, Project administration, Resources, Supervision, Validation, Visualization, Writing - original draft, Writing - review & editing.

Funding

The author(s) declare financial support was received for the research and/or publication of this article. Financial support from Grant PID2022-136462NB-I00 funded by "Ministerio de Ciencia e Innovación" and cofinanced by "European Union". TS and MG-B Acknowledge funding from the University of Virginia. JS-M acknowledges the predoctoral fellowship program of Junta de Castilla y León, co-funded by "Fondo Social Europeo" (Orden EDU875/2021). CT was supported by an Andrés Laguna fellowship (Junta de Castilla y León, co-financed by the Fondo Social Europeo Plus, FSE+; ORDEN EDU/300/2025).

Conflict of interest

JP is an employee of Cytognos, a BD Biosciences company Salamanca, Spain. MG-B is cofounder and has a significant equity stake in Circurna, Inc, which is commercializing RNA-based vaccines for emerging infections.

The remaining authors declare that the research was conducted in the absence of any commercial or financial relationships that could be construed as a potential conflict of interest.

The author CT declared that they were an editorial board member of Frontiers, at the time of submission. This had no impact on the peer review process and the final decision.

Generative Al statement

The author(s) declare that no Generative AI was used in the creation of this manuscript.

Any alternative text (alt text) provided alongside figures in this article has been generated by Frontiers with the support of artificial intelligence and reasonable efforts have been made to ensure accuracy, including review by the authors wherever possible. If you identify any issues, please contact us.

Publisher's note

All claims expressed in this article are solely those of the authors and do not necessarily represent those of their affiliated

organizations, or those of the publisher, the editors and the reviewers. Any product that may be evaluated in this article, or claim that may be made by its manufacturer, is not guaranteed or endorsed by the publisher.

Supplementary material

The Supplementary Material for this article can be found online at: https://www.frontiersin.org/articles/10.3389/fimmu.2025. 1693674/full#supplementary-material

References

- 1. Caravedo MA, Cabada MM. Human fascioliasis: current epidemiological status and strategies for diagnosis, treatment, and control. *Res Rep Trop Med.* (2020) 11:149–58. doi: 10.2147/RRTM.S237461
- 2. Lan Z, Zhang X-H, Xing J-L, Zhang A-H, Wang H-R, Zhang X-C, et al. Global prevalence of liver disease in human and domestic animals caused by Fasciola: A systematic review and meta-analysis. *J Global Health*. (2024) 14:4223. doi: 10.7189/jogh.14.04223
- 3. World Health Organization. Fasciola: background document for the WHO guidelines for drinking-water quality and the WHO guidelines on sanitation and health (2025). World Health Organization. Available online at: https://iris.who.int/handle/10665/380677 (Accessed October 14, 2025).
- 4. Fairweather I, Brennan GP, Hanna REB, Robinson MW, Skuce PJ. Drug resistance in liver flukes. *Int J Parasitology Drugs Drug Resistance*. (2020) 12:39–59. doi: 10.1016/j.ijpddr.2019.11.003
- 5. Pacheco IL, Abril N, Zafra R, Molina-Hernández V, Morales-Prieto N, Bautista MJ, et al. Fasciola hepatica induces Foxp3 T cell, proinflammatory and regulatory cytokine overexpression in liver from infected sheep during early stages of infection. *Veterinary Res.* (2018) 49:56. doi: 10.1186/s13567-018-0550-x
- 6. Donnelly S, O'Neill SM, Sekiya M, Mulcahy G, Dalton JP. Thioredoxin peroxidase secreted by fasciola hepatica induces the alternative activation of macrophages. *Infection Immun.* (2005) 73:166–73. doi: 10.1128/iai.73.1.166-173.2005
- 7. Donnelly S, Stack CM, O'Neill SM, Sayed AA, Williams DL, Dalton JP. Helminth 2-Cys peroxiredoxin drives Th2 responses through a mechanism involving alternatively activated macrophages. FASEB journal: Off Publ Fed Am Societies Exp Biol. (2008) 22:4022–32. doi: 10.1096/fj.08-106278
- 8. Ryan S, Shiels J, Taggart CC, Dalton JP, Weldon S. Fasciola hepatica-derived molecules as regulators of the host immune response. *Front Immunol.* (2020) 11:2182. doi: 10.3389/fimmu.2020.02182
- 9. Pleasance J, Wiedosari E, Raadsma HW, Meeusen E, Piedrafita D. Resistance to liver fluke infection in the natural sheep host is correlated with a type-1 cytokine response. *Parasite Immunol.* (2011) 33:495–505. doi: 10.1111/j.1365-3024.2011.01305.x
- 10. Martínez-Fernández AR, Nogal-Ruiz JJ, López-Abán J, Ramajo V, Oleaga A, Manga-González Y, et al. Vaccination of mice and sheep with Fh12 FABP from Fasciola hepatica using the new adjuvant/immunomodulator system ADAD. *Veterinary Parasitol.* (2004) 126:287–98. doi: 10.1016/j.vetpar.2004.07.023
- 11. López-Abán J, Nogal-Ruiz JJ, Vicente B, Morrondo P, Diez-Baños P, Hillyer GV, et al. The addition of a new immunomodulator with the adjuvant adaptation ADAD system using fatty acid binding proteins increases the protection against Fasciola hepatica. Veterinary Parasitol. (2008) 153:176–81. doi: 10.1016/j.vetpar.2008.01.023
- 12. Golden O, Flynn RJ, Read C, Sekiya M, Donnelly SM, Stack C, et al. Protection of cattle against a natural infection of *Fasciola hepatica* by vaccination with recombinant cathepsin L1 (rFhCL1). *Vaccine*. (2010) 28:5551–7. doi: 10.1016/j.vaccine.2010.06.039
- 13. Maggioli G, Bottini G, Basika T, Alonzo P, Salinas G, Carmona C. Immunization with Fasciola hepatica thioredoxin glutathione reductase failed to confer protection against fasciolosis in cattle. Veterinary Parasitol. (2016) 224:13–9. doi: 10.1016/j.vetpar.2016.05.007
- 14. Zafra R, Buffoni L, Pérez-Caballero R, Molina-Hernández V, Ruiz-Campillo MT, Pérez J, et al. Efficacy of a multivalent vaccine against Fasciola hepatica infection in sheep. *Veterinary Res.* (2021) 52:13. doi: 10.1186/s13567-021-00895-0
- 15. Meyer F, Meyer H, Bueding E. Lipid metabolism in the parasitic and free-living flatworms, Schistosoma mansoni and Dugesia dorotocephala. *Biochim Et Biophys Acta*. (1970) 210:257–66. doi: 10.1016/0005-2760(70)90170-0
- 16. Casanueva R, Hillyer GV, Ramajo V, Oleaga A, Espinoza EY, Muro A. Immunoprophylaxis against Fasciola hepatica in rabbits using a recombinant Fh15

fatty acid-binding protein. J Parasitol. (2001) 87:697–700. doi: 10.1645/0022-3395 (2001)087[0697:IAFHIR]2.0.CO;2

- 17. Vicente B, López-Abán J, Rojas-Caraballo J, Pérez del Villar L, Hillyer GV, Martínez-Fernández AR, et al. A Fasciola hepatica-derived fatty acid binding protein induces protection against schistosomiasis caused by Schistosoma bovis using the adjuvant adaptation (ADAD) vaccination system. *Exp Parasitol.* (2014) 145:145–51. doi: 10.1016/j.exppara.2014.08.007
- 18. Vicente B, López-Abán J, Rojas-Caraballo J, del Olmo E, Fernández-Soto P, Ramajo-Martín V, et al. The combination of the aliphatic diamine AA0029 in ADAD vaccination system with a recombinant fatty acid binding protein could be a good alternative for the animal schistosomiasis control. *Exp Parasitol.* (2015) 154:134–42. doi: 10.1016/j.exppara.2015.04.022
- 19. López-Abán J, Casanueva P, Nogal J, Arias M, Morrondo P, Diez-Baños P, et al. Progress in the development of *Fasciola hepatica* vaccine using recombinant fatty acid binding protein with the adjuvant adaptation system ADAD. *Veterinary Parasitol.* (2007) 145:287–96. doi: 10.1016/j.vetpar.2006.12.017
- 20. Rosado-Franco JJ, Armina-Rodriguez A, Marzan-Rivera N, Burgos AG, Spiliopoulos N, Dorta-Estremera SM, et al. Recombinant fasciola hepatica fatty acid binding protein as a novel anti-inflammatory biotherapeutic drug in an acute gramnegative nonhuman primate sepsis model. *Microbiol Spectr.* (2021) 9:e01910–21. doi: 10.1128/Spectrum.01910-21
- 21. Versteeg L, Almutairi MM, Hotez PJ, Pollet J. Enlisting the mRNA vaccine platform to combat parasitic infections. *Vaccines*. (2019) 7:122. doi: 10.3390/vaccines7040122
- 22. De Oliveira AS, Versteeg L, Briggs N, Adhikari R, Villar MJ, Redd JR, et al. Altering the intracellular trafficking of Necator americanus GST-1 antigen yields novel hookworm mRNA vaccine candidates. *PloS Negl Trop Dis.* (2025) 19:12809. doi: 10.1371/journal.pntd.0012809
- 23. Sánchez-Montejo J, Strilets T, Manzano-Román R, López-Abán J, García-Blanco MA, Vicente B, et al. Design and Expression of Fasciola hepatica Multiepitope Constructs Using mRNA Vaccine Technology. *Int J Mol Sci.* (2025) 26:1190. doi: 10.3390/ijms26031190
- 24. Holtkamp S, Kreiter S, Selmi A, Simon P, Koslowski M, Huber C, et al. Modification of antigen-encoding RNA increases stability, translational efficacy, and T-cell stimulatory capacity of dendritic cells. *Blood*. (2006) 108:4009–17. doi: 10.1182/blood-2006-04-015024
- 25. Orlandini von Niessen AG, Poleganov MA, Rechner C, Plaschke A, Kranz LM, Fesser S, et al. Improving mRNA-based therapeutic gene delivery by expression-augmenting 3' UTRs identified by cellular library screening. *Mol Therapy: J Am Soc Gene Ther.* (2019) 27:824–36. doi: 10.1016/j.ymthe.2018.12.011
- Trepotec Z, Geiger J, Plank C, Aneja MK, Rudolph C. Segmented poly(A) tails significantly reduce recombination of plasmid DNA without affecting mRNA translation efficiency or half-life. RNA (New York N.Y.). (2019) 25:507–18. doi: 10.1261/rna.069286.118
- 27. Baiersdörfer M, Boros G, Muramatsu H, Mahiny A, Vlatkovic I, Sahin U, et al. A Facile Method for the Removal of dsRNA Contaminant from *In Vitro*-Transcribed mRNA. *Mol Ther Nucleic Acids.* (2019) 15:26–35. doi: 10.1016/j.omtn.2019.02.018
- 28. Sabnis S, Kumarasinghe ES, Salerno T, Mihai C, Ketova T, Senn JJ, et al. A novel amino lipid series for mRNA delivery: improved endosomal escape and sustained pharmacology and safety in non-human primates. *Mol Ther*. (2018) 26:1509–19. doi: 10.1016/j.ymthe.2018.03.010
- 29. R Core Team. *R: A Language and Environment for Statistical Computing* (2024). Vienna, Austria: R Foundation for Statistical Computing. Available online at: https://www.R-project.org/.
- 30. Wickham H. ggplot2: Elegant Graphics for Data Analysis (2016). Springer-Verlag New York. Available online at: https://ggplot2.tidyverse.org.

31. Shi C, Jia T, Mendez-Ferrer S, Hohl TM, Serbina NV, Lipuma L, et al. Bone marrow mesenchymal stem and progenitor cells induce monocyte emigration in response to circulating toll-like receptor ligands. *Immunity*. (2011) 34:590–601. doi: 10.1016/j.immuni.2011.02.016

- 32. Verbeke R, Hogan MJ, Loré K, Pardi N. Innate immune mechanisms of mRNA vaccines. *Immunity*. (2022) 55:1993–2005. doi: 10.1016/j.immuni.2022.10.014
- 33. Thess A, Grund S, Mui BL, Hope MJ, Baumhof P, Fotin-Mleczek M, et al. Sequence-engineered mRNA without chemical nucleoside modifications enables an effective protein therapy in large animals. *Mol Ther.* (2015) 23:1456–64. doi: 10.1038/mt.2015.103
- 34. van den Bossche WBL, Rykov K, Teodosio C, ten Have BLEF, Knobben BAS, Sietsma MS, et al. Flow cytometric assessment of leukocyte kinetics for the monitoring of tissue damage. *Clin Immunol.* (2018) 197:224–30. doi: 10.1016/j.clim.2018.09.014
- 35. Wong KL, Tai JJ-Y, Wong W-C, Han H, Sem X, Yeap W-H, et al. Gene expression profiling reveals the defining features of the classical, intermediate, and nonclassical human monocyte subsets. *Blood.* (2011) 118:e16–31. doi: 10.1182/blood-2010-12-326355
- 36. Williams H, Mack C, Baraz R, Marimuthu R, Naralashetty S, Li S, et al. Monocyte differentiation and heterogeneity: inter-subset and interindividual differences. *Int J Mol Sci.* (2023) 24:8757. doi: 10.3390/ijms24108757
- 37. Royo J, Rahabi M, Kamaliddin C, Ezinmegnon S, Olagnier D, Authier H, et al. Changes in monocyte subsets are associated with clinical outcomes in severe malarial anaemia and cerebral malaria. *Sci Rep.* (2019) 9:17545. doi: 10.1038/s41598-019-52579-7
- 38. Swirski FK, Nahrendorf M, Etzrodt M, Wildgruber M, Cortez-Retamozo V, Panizzi P, et al. Identification of splenic reservoir monocytes and their deployment to inflammatory sites. *Sci (New York N.Y.).* (2009) 325:612–6. doi: 10.1126/science.1175202
- 39. Martín-Fontecha A, Thomsen LL, Brett S, Gerard C, Lipp M, Lanzavecchia A, et al. Induced recruitment of NK cells to lymph nodes provides IFN-gamma for T(H)1 priming. *Nat Immunol.* (2004) 5:1260–5. doi: 10.1038/ni1138
- 40. Farsakoglu Y, Palomino-Segura M, Latino I, Zanaga S, Chatziandreou N, Pizzagalli DU, et al. Influenza vaccination induces NK-cell-mediated type-II IFN

- response that regulates humoral immunity in an IL-6-dependent manner. Cell Rep. (2019) 26:2307–15. doi: 10.1016/j.celrep.2019.01.104
- 41. Milush JM, Mir KD, Sundaravaradan V, Gordon SN, Engram J, Cano CA, et al. Lack of clinical AIDS in SIV-infected sooty mangabeys with significant CD4+ T cell loss is associated with double-negative T cells. *J Clin Invest.* (2011) 121:1102–10. doi: 10.1172/JC144876
- 42. Mou Z, Liu D, Okwor I, Jia P, Orihara K, Uzonna JE. MHC class II restricted innate-like double negative T cells contribute to optimal primary and secondary immunity to Leishmania major. *PloS Pathog.* (2014) 10:1004396. doi: 10.1371/journal.ppat.1004396
- 43. Torben W, Molehin AJ, Blair RV, Kenway C, Shiro F, Roslyn D, et al. The self-curing phenomenon of schistosome infection in rhesus macaques: insight from *in vitro* studies. *Ann New York Acad Sci.* (2017) 1408:79–89. doi: 10.1111/nyas.13565
- 44. Alameh M-G, Tombácz I, Bettini E, Lederer K, Ndeupen S, Sittplangkoon C, et al. Lipid nanoparticles enhance the efficacy of mRNA and protein subunit vaccines by inducing robust T follicular helper cell and humoral responses. *Immunity.* (2021) 54:2877–2892.e7. doi: 10.1016/j.immuni.2021.11.001
- 45. Walsh KP, Brady MT, Finlay CM, Boon L, Mills KHG. Infection with a helminth parasite attenuates autoimmunity through TGF-beta-mediated suppression of Th17 and Th1 responses. *J Immunol (Baltimore Md.: 1950)*. (2009) 183:1577–86. doi: 10.4049/jimmunol.0803803
- 46. Besin G, Milton J, Sabnis S, Howell R, Mihai C, Burke K, et al. Accelerated blood clearance of lipid nanoparticles entails a biphasic humoral response of B-1 followed by B-2 lymphocytes to distinct antigenic moieties. *ImmunoHorizons*. (2019) 3:282–93. doi: 10.4049/immunohorizons.1900029
- 47. Lederer K, Castaño D, Gómez Atria D, Oguin TH, Wang S, Manzoni TB, et al. SARS-coV-2 mRNA vaccines foster potent antigen-specific germinal center responses associated with neutralizing antibody generation. *Immunity*. (2020) 53:1281–95. doi: 10.1016/j.immuni.2020.11.009
- 48. Rufino-Moya PJ, Zafra Leva R, Gonçalves Reis LDP, Acosta García I, Ruiz Di Genova D, Sánchez Gómez A, et al. Prevalence of gastrointestinal parasites in small ruminant farms in southern Spain. *Animals*. (2024) 14:1668. doi: 10.3390/ani14111668